

Reflectance and thermorefectance studies of CrCl_3 , CrBr_3 , NiCl_2 , and NiBr_2 crystals

G. Guizzetti,* L. Nosenzo,* I. Pollini,[†] E. Reguzzoni,* G. Samoggia,* and G. Spinolo[†]

Gruppo Nazionale di Struttura della Materia del Consiglio Nazionale delle Ricerche, Italy

(Received 29 April 1976)

Reflectance spectra at 300 and 80 K and thermorefectance spectra at 80 and 30 K are shown for CrCl_3 , CrBr_3 , NiCl_2 , and NiBr_2 in the energy range 2–10 eV. A general consistency was found between the two types of data. The temperature-shift coefficients of the various peaks have been found to be positive in nickel halides, while in chromium compounds were negative as usual. Through the combined analysis of the two types of experiments, it has been possible to distinguish the transitions of “charge transfer” character from those of excitonic and band-to-band origin. A discussion of the various possible charge-transfer processes has also been made.

I. INTRODUCTION

In the present paper we report on a study of the optical-reflectivity spectra of CrCl_3 and CrBr_3 and thermorefectivity spectra of CrCl_3 , CrBr_3 , NiCl_2 , and NiBr_2 , in the same high-extinction-coefficient region. The optical-reflectivity spectra of NiCl_2 and NiBr_2 from 2 to 10 eV have been published recently¹ and an interpretation scheme has been proposed.

Our aim is to locate the $d-d$ crystal-field transitions in the energy gap of transition-metal halides and obtain a better understanding of the charge-transfer and band-to-band transitions in relation to the electronic band structure. A similar effort is being made and is in a more advanced stage for the transition-metal dichalcogenides.²⁻⁴ It seems of interest to try to have a unique approach for the study of the optical properties of the two classes of transition-metal compounds just mentioned. In this frame, the localization of d electrons or, in other words, the ionicity of the anion-cation bonds should be the main factors for determining the optical and electrical properties of these materials.

CrCl_3 and CrBr_3 are magnetic insulators with hexagonal layer structure; the metal is contained in a trigonally distorted octahedron of halogen ions. Magnetic and crystallographic data on them may be found in a paper by Dillon, Kamimura, and Remeika,⁵ which mainly deals with the specific magnetic rotation in the charge-transfer edge. The optical absorption⁵⁻⁷ and photoconductivity,^{7,8} in the crystal-field region have also been studied. With detailed measurements of specific magnetic rotation⁹ and cubic and trigonal field parameters and the spin-orbit coefficient have also been evaluated. While the crystal-field region is rather well studied, the charge-transfer and band-to-band transitions have received less attention even though proposals for assignment of the charge-

transfer edge^{5,7,10} and of the first charge-transfer peaks found in absorption measurements on films⁷ have been made.

NiCl_2 and NiBr_2 are antiferromagnetic insulators with the hexagonal CdCl_2 structure; the local field around Ni^{2+} has O_h symmetry. The Néel temperatures for NiCl_2 and NiBr_2 are 50 and 60 K, respectively. These materials have already been studied: the absorption spectrum in the crystal-field region¹¹ and the reflectivity¹ up to 10 eV are known in considerable detail. Optical absorption on films has been carried out up to 40 eV;¹² x-ray photoemission spectra of the valence electrons¹³ are also present in the literature.

With the data shown in Sec. II we will be in the position to give for all the crystals considered an explanation of the charge-transfer spectra found in the spectral region 2–3 to 6–7 eV. The discussion is carried out in Sec. III.

II. EXPERIMENTAL

A. Sample preparation and experimental technique

CrCl_3 and CrBr_3 crystals were prepared in our laboratories with the flow-system method at the temperature of 960 and 750 °C, respectively; the crystal thicknesses of these mica-like platelets of average area $\approx 0.8 \text{ cm}^2$ range from 5 to 50 μm . The crystals of CrCl_3 and of CrBr_3 appear, respectively, pink violet and dark green; they are lustrous and easy to handle. NiCl_2 and NiBr_2 crystals were prepared with the same method at temperatures of 700 and 600 °C, respectively, and present thicknesses and sizes of the same order as the chromium halide samples. Colors are gold yellow (NiCl_2) and yellow brown (NiBr_2). The crystals are shiny, somewhat hygroscopic, and require careful handling in a dry atmosphere.

The double-beam optical-reflectivity apparatus features a Hinteregger hydrogen-discharge lamp model 630, supplied by McPherson, a McPherson

vacuum monochromator model 218 and homemade stainless-steel double-vessel cryostat. A thin crystal (≈ 0.5 mm) of LiF used as a beam splitter, separates the incident radiation in the reference and reflected beams, which are collected by two EMI 9526SQ photomultipliers. The electrical signals are converted into the logarithm of their ratio and the spectra are continuously recorded. In the vacuum uv region, freshly prepared sodium salicylate light converters are used.

The quasinormal incidence spectra reported were repeated several times to check the reproducibility, and always obtained on freshly grown crystals. The effect of contamination of the surface (the pressure in the cryostat was of the order of 10^{-7} Torr and two cold traps were mounted in the vacuum line) was checked, particularly at low temperatures, by repeatedly obtaining the reflectivity spectrum. Changes were found to be negligible after 1 h, whereas the average time to get a complete scan from 2 to 10 eV was about 15 min.

The main features of the thermorefectance apparatus have been described elsewhere.¹⁴ The temperature of the sample was modulated by using indirect heating. The germanium heater was fastened to the cold finger of the optical cryostat. The thin platelets, just after being cleaved, were pressed to the Ge heater by two springs. Temperature modulation of the order of 1 K was used in all the reported measurements. In the sample chamber the vacuum was $\approx 5 \times 10^{-9}$ Torr. Also the thermorefectance curves were reproducible.

For calculating the dielectric constants $\epsilon_1(E)$ and $\epsilon_2(E)$ in the case of CrCl_3 and CrBr_3 we had at our disposal only our reflectivity data between 2 and 10 eV. In this case we have extrapolated $R(E')$ at high energies ($E' \geq E_2$) with a tail¹⁵:

$$R(E') = R_2(E_2/E')^m, \quad R_2 = R(E_2), \quad E_2 = 10 \text{ eV}.$$

At low energies ($E' < 2$ eV), where the absorption coefficient is nearly zero, we have calculated $R(E')$ from the values of n obtained by means of the interference fringes technique,⁷ and by imposing the continuity of the derivative at $E' = 2$ eV. Then, the phase $\theta(E)$ was calculated in a customary way.¹⁵

In the case of nickel halides, we had at disposal not only our data on the reflectivity ($2 \leq E' \leq 10$ eV), but also the absorption coefficient for thin films from 1 to 40 eV,¹² so we could proceed in the following way:

(i) We used¹² $\alpha(E')$ for calculating $n(E)$ (for $E > 10$ eV), taking¹⁵

$$n(E) = 1 + \frac{1}{\pi} \text{P} \int_0^{E_3} \frac{C\alpha(E')}{E'^2 - E^2} dE',$$

where $\alpha(E')$ beyond 40 eV has been assumed to behave as

$$\alpha(E') = \alpha_2(E_2/E')^m,$$

$$E_2 = 40 \text{ eV for NiBr}_2,$$

$$E_2 = 35 \text{ eV for NiCl}_2.$$

We have chosen the parameter m and the upper value of the integral, $E_3 > E_2$, so as to avoid discontinuity at E_2 and to fit reflectivity data in the low-absorption region.¹⁶ (ii) Then, from α and n we can calculate $R(E)$ in the region beyond our experimental data. (iii) From the knowledge of $R(E)$ from zero to E_3 we have been able to determine the optical functions ϵ_1 , ϵ_2 , n , k , $\text{Im}\tilde{\epsilon}$, ϵ_{off} , and n_{off} from Kramers-Krönig transforms.¹⁵

Let us remark that the published data on α for¹² NiBr_2 give values of $R \sim 10\%$ greater than ours in a systematic way. Probably this discrepancy could be due to the nature of the films used in the measurements of $\alpha(E)$. This discrepancy has been resolved by introducing a correction factor in $\alpha(E)$.

A change in choosing m and E_3 affects the values of the optical constants but not the positions of the structures observed in the measurement region; specifically, the energy peaks of ϵ_2 , which give the energy of the transitions, should be considered quite correct.

The calculation of n_{off} and ϵ_{off} has been performed by using the sum rules¹⁷

$$\begin{aligned} n_{\text{off}}(E) &= \frac{m}{2M^2\hbar^2Ne} \int_0^E E' \epsilon_2(E') dE', \\ \epsilon_{\text{off}}(E) &= 1 + \frac{2}{\pi} \int_0^E \frac{\epsilon_2(E')}{E'} dE', \end{aligned} \quad (1)$$

where N is the atomic density.

B. Experimental results

In Figs. 1(a) and 2(a), 300- and 80-K reflectivity spectra of CrCl_3 and CrBr_3 are shown.

The spectra may be divided into two parts; the first, up to the deep minimum of reflectivity located at ≈ 6.9 eV for CrBr_3 and at ≈ 7.8 eV for CrCl_3 , and the second beyond that minimum. The first part of the spectrum is rather similar for both crystals, in fact we notice that in both CrCl_3 and CrBr_3 there is a strongly reflecting region and a low-reflection region, rather structured. In the strongly reflecting region two clearly distinct peaks show up in CrBr_3 and a broader peak, with a hump at 3.6 eV and a knee at 5.1 eV appears in CrCl_3 . In the part of the spectra at energies higher than the deep minimum, CrBr_3 shows two peaks at ≈ 7.3 and 8.2 eV. Analogous structures cannot be found in CrCl_3 .

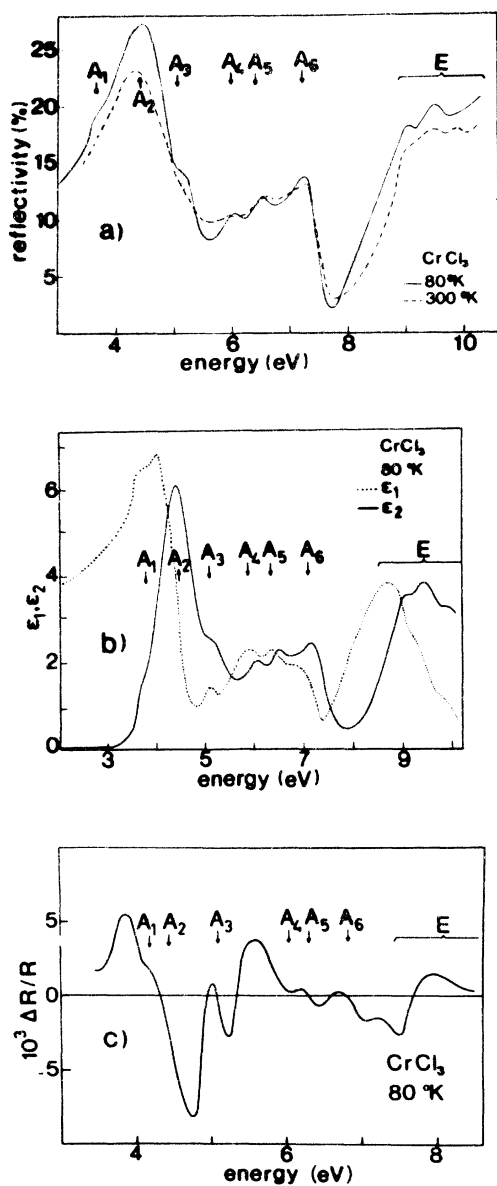


FIG. 1. (a) CrCl_3 reflectivity spectrum at 80 and 300 K. (b) Real and imaginary parts of the dielectric constant of CrCl_3 obtained from 80-K reflectivity data. (c) Thermoreflectance of CrCl_3 at 80 K.

A similar situation has also been found in NiCl_2 and NiBr_2 [see Figs. 3(a) and 4(a)]. Moreover, in nickel halides the high-energy region of the reflectivity spectra of NiBr_2 is certainly more structured than the corresponding region of NiCl_2 . The energy positions of all the peaks and structures are collected in Tables I and II. For all the crystals, the data above 9 eV should be regarded as tentative since in that region the monochromator has an higher percentage of stray light.

We performed the Kramers-Krönig analysis of

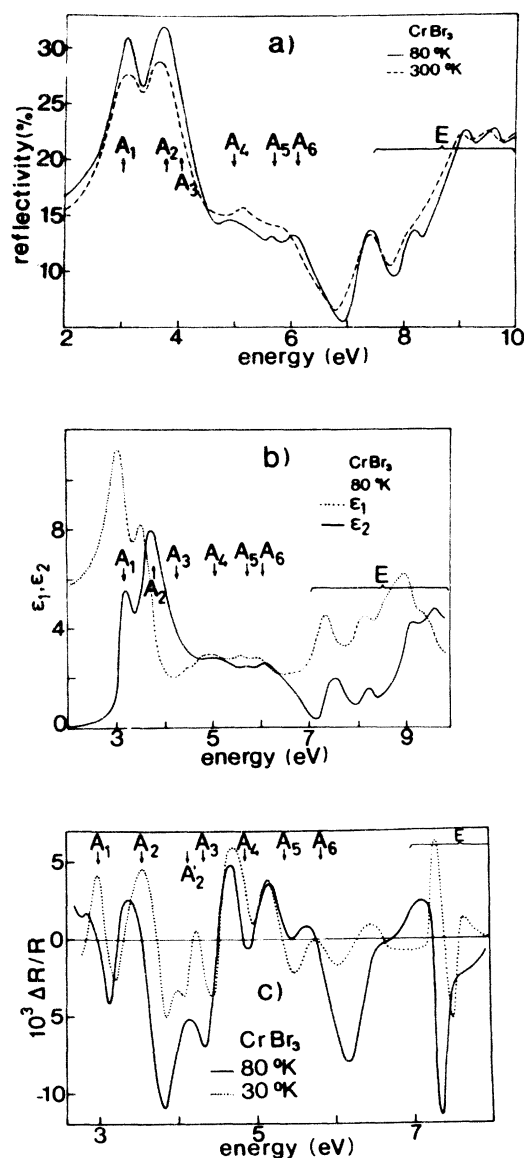


FIG. 2. (a) CrBr_3 reflectivity spectrum at 80 and 300 K. (b) Real and imaginary parts of the dielectric constant of CrBr_3 obtained from 80-K reflectivity data. (c) Thermoreflectance of CrBr_3 at 80 and 30 K.

our reflectivity spectra and the $\epsilon_1(E)$ and $\epsilon_2(E)$ curves calculated from 80-K data are reported for all the crystals studied in Figs. 1(b) to 4(b). It is quite satisfying to observe that $\epsilon_2(E)$ for NiCl_2 and NiBr_2 reproduces the absorption data on films¹² as well as it could be reasonably expected. Due to the fact that these materials are hygroscopic, measurements involving the surface should be critically considered. For chromium halides a similar check is not possible but, fortunately, they are not hygroscopic.

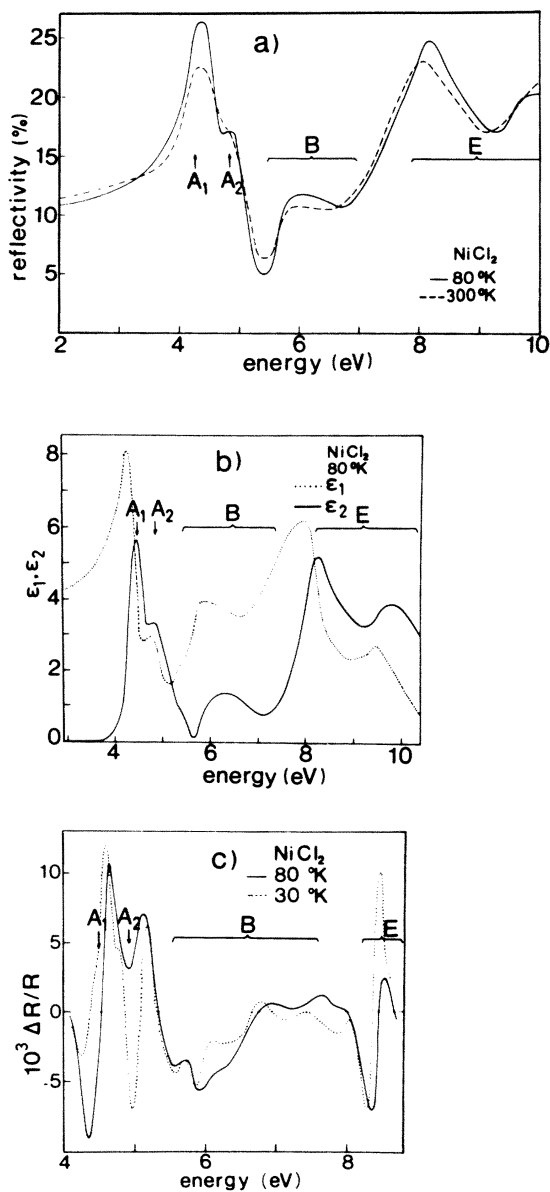


FIG. 3. (a) NiCl_2 reflectivity spectrum at 80 and 300 K. (b) Real and imaginary parts of the dielectric constant of NiCl_2 obtained from 80-K reflectivity data. (c) Thermoreflectance of NiCl_2 at 80 and 30 K.

In Figs. 1(c) to 4(c) the thermoreflectivity (TR) spectra of CrCl_3 and CrBr_3 , NiCl_2 and NiBr_2 , taken at 30 and 80 K are reported. In these spectra we can find structures corresponding to the reflectivity ones. For example, the two peaks at 3.10 and 3.74 eV observed in the reflectivity spectrum of CrBr_3 at 80 K correspond to the structures at 3.00 and 3.56 eV found in the 80-K TR spectrum. However, finer details are observed in thermoreflectivity: we can notice, in fact, that where, around 4.3 eV, a slight change in slope is

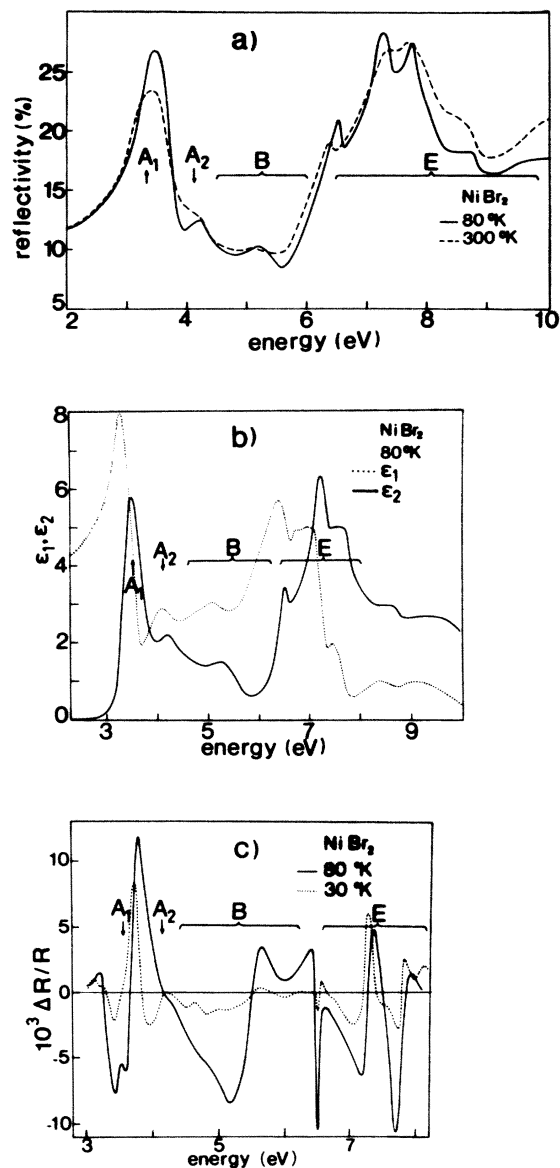


FIG. 4. (a) NiBr_2 reflectivity spectrum at 80 and 300 K. (b) Real and imaginary parts of the dielectric constant of NiBr_2 obtained from 80-K reflectivity data. (c) Thermoreflectance of NiBr_2 at 80 and 30 K.

observed in the 80-K reflectivity spectrum of CrBr_3 , a couple of well-resolved structures appear in the 30-K TR spectrum.

In order to evaluate the information obtained from thermoreflectivity it is useful to remember¹⁸ that the temperature modulation does not yield a strict derivative spectrum (as wavelength modulation would) since it is an "internal" modulation and involves the effect of temperature on the optical constants. However in the following we shall assume that the broadening term is small com-

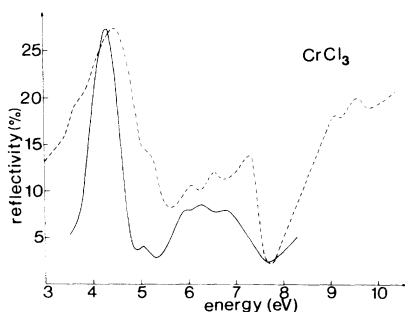


FIG. 5. Comparison between the CrCl_3 reflectivity spectrum (dashed line) and the integrated TR spectrum (solid line) at 80 K.

that, while crystals-field transitions of rare-earth and transition-metal ions are quite well understood, a comprehensive view of the charge-transfer, orbital-promotion, and band-to-band transitions is lacking.

The situation is rather the same in transition-metal halides and we will not go beyond a qualitative discussion in commenting the optical spectra here reported. With reference to a rigid-band scheme of the electronic structure of transition-metal halides one observes that at energies higher than crystal-field transitions one has to arrange a number of different kinds of transitions: (i) the transitions from the valence band (mostly p -halogen character) to the levels localized on the metal ion, which are called "charge transfer." With reference to the electronic configuration they could be described as $p^6(\text{halogen})3d^n \rightarrow p^5(\text{halogen})3d^{n+1}$ or also $p^6(\text{halogen})3d^n \rightarrow p^5(\text{halogen})3d^{n+1}4s^1$; (ii) the transitions from the $3d$ levels to the conduction band ($4s$ and $4p$ metal levels), which are called orbital-promotion transitions: $3d^n \rightarrow 3d^{n-1}4s$, $3d^{n-1}4p$; (iii) the transitions from the valence band to the conduction band, which are called interband transitions.

The relative location in energy of these various sets of transitions is still not known. Adler and Feinleib²² have suggested that in some metal oxide charge-transfer transitions could be higher in energy than orbital-promotion and band-to-band transitions. We think, however, that our spectra rise mostly from charge-transfer transitions, on the ground of the following considerations:

(i) It has been shown⁵ that the large specific magnetic rotation observed at the edge of the strong absorbing region in chromium halides is associated with charge-transfer transitions in which one electron in a halide orbital is raised into an orbital localized on the chromium ion.

(ii) As it is shown in Fig. 6, n_{eff} calculated by Eq. (1) using the α values of Sakisaka, Ishii, and Sagawa¹² up to 40 eV for the nickel halides

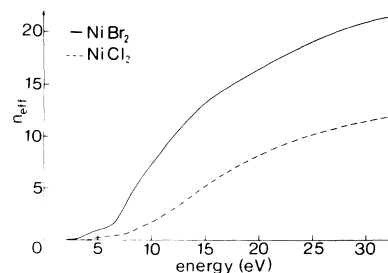


FIG. 6. n_{eff} obtained for NiBr_2 and NiCl_2 by the sum rules of Eq. (1). 300-K data are used.

reaches in the first part of the spectrum a nearly steady value of about 1.0 for both crystals. At nearly 6.5 eV (NiBr_2) and 8.0 eV (NiCl_2), n_{eff} begins to jump up to very high values reaching 11 for NiCl_2 and 22 for NiBr_2 . We think that the region of low values of n_{eff} defines quite well the charge transfer region. In fact due to the small overlapping between the halogen and the d -metal wave functions, charge-transfer transitions are allowed, but weaker than $d \rightarrow p$ intraionic or band-to-band transitions. The sudden increase of n_{eff} could mark the beginning of band-to-band and orbital promotion transitions. The saturation value of n_{eff} at 35 eV probably marks the exhaustion of the oscillator strengths of the optical transitions of the $12p$ valence electrons of the NiX_2 molecule plus the $8d$ electrons of the metal. Other transitions do not exist in this region since the transitions that involve deep d levels of the Br ion fall at 80 eV.²³ A very small error in the measurement of the α coefficient (for example in the measurement of the thickness of the film) could account for the discrepancy between n_{eff} and the number of electrons at disposal.

(iii) Let us now observe the shape and behavior of the $\Delta R/R$ structures in nickel salts: The main A_1 and A_2 structures have a linewidth of ≈ 0.30 eV at 80 K and an absorptionlike shape, while the structure at the beginning of the region called E has a line width ≈ 0.05 eV in NiBr_2 and ≈ 0.1 eV in NiCl_2 and a dispersionlike shape. The fact that we have a narrower linewidth at high energies suggests associating the E transitions with a different electronic process with respect to A_1 and A_2 and specifically with an exciton bound to the valence-conduction band gap.

Coming now to more detailed analysis of the charge-transfer peaks, denoted A_i in the figures, we should decide to which electronic configuration they belong and which are the symmetries of the individual final states.

We must consider either $p^5(\text{halogen})3d^{n+1}$ and/or $p^5(\text{halogen})3d^n4s^1$ as final configurations, which

could have nearly the same energy. Actually the far-ultraviolet absorption spectrum of NiO has been well interpreted on the basis of two nearly-degenerate configurations $p^5(\text{metal})3d^9$ and $p^5(\text{metal})3d^84s^1$.²⁴ To proceed in our rough discussion let us suppose that the interaction between the hole and the outer electrons ($3d^{n+1}$ or $3d^n4s^1$) may be disregarded because of the delocalization of the hole. In this approximation two possibilities should be considered. If the charge-transfer spectra arise from $3d^n \rightarrow p^5(\text{halogen})3d^{n+1}4s^1$ transitions, owing to the full symmetry of the s wave function, they would be comparable with the $d-d$ spectra, as it has been suggested previously.¹ In the case of $3d^n \rightarrow p^5(\text{halogen})3d^{n+1}$ transitions the spectra would reflect the multiplicity of the $3d^{n+1}$ final states.

Let us consider now the optical spectra of nickel-halide crystals. Two well-defined structures A_1 and A_2 are resolved both in thermoreflectivity and in reflectivity. The broad B region, which is structureless at 80 K in reflectivity and TR spectra, displays some faint oscillations in the 30-K TR spectrum. The ground state of nickel salts has ${}^3A_{2g}$ symmetry, then only transitions to ${}^3T_{2u}$ states are allowed. Only two ${}^3T_{2u}$ states are obtained from the configuration $p(\text{hole})d^9$, the first one by coupling the $t_{1u}(\sigma)$ hole with the e_g electron state and the second one by coupling with the t_{2g} state. By attributing the A_1 and A_2 bands to these states, the energy separation $A_1 - A_2$ (about 0.4 eV in NiCl_2 and 0.7 eV in NiBr_2) could measure the crystal-field separation modified by the electron-hole interaction. One may then wonder

about the origin of the weak B structures and attempt an interpretation in terms of some new kind of transitions. In an alternative way, if one assumes that the $p^5(\text{halogen})3d^84s^1$ configuration is lower in energy than the $p^5(\text{halogen})3d^9$ one, a large number of transitions are allowed and all the A_i and B structures could be assigned.¹

In the case of chromium salts, let us assume that the final states arise from the $p^5(\text{halogen})3d^4$ configuration. In order to attribute the well-defined peaks to specific transitions, we suppose that the energy sequence of final states is, neglecting the electron-hole interaction, the same as the one characterizing the d^{n+1} states as calculated by Tanabe-Sugano.²³ Then, to calculate the final-state symmetry we multiply the $t_{1u}^h(\sigma)$ representation of the valence hole by the irreducible representations d^{n+1} and reduce the product representation into its irreducible components. In the case of chromium halides the ground state has ${}^2A_{2g}$ symmetry and only transitions to ${}^4T_{2u}$ levels are allowed. From the diagrams of Ref. 23 transitions from the ${}^4A_{2g}$ ground state to the ${}^5E_g(d^4) \times {}^2T_{1u}(\sigma)$, ${}^5T_{2g}(d^4) \times {}^2T_{1u}(\sigma)$, ${}^3T_{1g}(d^4) \times {}^2T_{1u}(\sigma)$, ${}^3E_g(d^4) \times {}^2T_{1u}(\sigma)$, ${}^3T_{1g}(d^4) \times {}^2T_{1u}(\sigma)$, and ${}^3T_{2g}(d^4) \times {}^2T_{1u}(\sigma)$ final states are allowed and they could be correlated to the A_1 up to A_6 structures, respectively, shown in reflectivity and TR spectra. If one compares the energies of the assigned transitions with the Tanabe-Sugano tables, one observes that the relative spacings are not preserved. Probably one might obtain a better agreement by correctly taking into account the interaction energy between the d electron and the hole.

*Istituto di Fisica dell'Università di Pavia, Pavia, Italy.

†Istituto di Fisica dell'Università di Milano, Milano, Italy.

¹I. Pollini and G. Spinolo, *J. Phys. C* **7**, 2391 (1974).

²I. A. Wilson and A. D. Yoffe, *Adv. Phys.* **18**, 193 (1969).

³L. F. Mattheiss, *Phys. Rev. Lett.* **30**, 784 (1973).

⁴R. V. Kasowski, *Phys. Rev. Lett.* **30**, 1175 (1973).

⁵J. F. Dillon, Jr., H. Kamimura, and J. P. Remeika, *J. Phys. Chem. Solids* **27**, 1531 (1966).

⁶D. L. Wood, J. Ferguson, K. Knox, and J. F. Dillon, Jr., *J. Chem. Phys.* **39**, 890 (1963).

⁷I. Pollini and G. Spinolo, *Phys. Status Solidi* **41**, 691 (1970).

⁸K. K. Kanazawa and G. B. Street, *Phys. Status Solidi* **38**, 445 (1970).

⁹C. Limido, G. Pedroli, and G. Spinolo, *Solid State Commun.* **11**, 1385 (1972).

¹⁰W. Jung, *J. Appl. Phys.* **36**, 2422 (1965).

¹¹M. Kozielski, I. Pollini, and G. Spinolo, *J. Phys. C* **5**, 1253 (1972).

¹²Y. Sakisaka, T. Ishii, and T. Sagawa, *J. Phys. Soc.*

Jpn. **36**, 1365 (1974).

¹³Y. Sakisaka, T. Ishii, and T. Sagawa, *J. Phys. Soc. Jpn.* **36**, 1372 (1974).

¹⁴G. Guizzetti, L. Nosenzo, E. Reguzzoni, and G. Samoggia, *Phys. Rev. B* **9**, 640 (1974).

¹⁵F. Stern, in *Solid State Physics*, edited by F. Seitz and D. Turnbull (Academic, New York, 1968), Vol. 15, p. 331.

¹⁶R. S. Bauer, W. E. Spicer, and J. T. Whitte, III, *J. Opt. Soc. Am.* **64**, 830 (1974).

¹⁷H. R. Philipp and H. Ehrenreich, *Phys. Rev.* **129**, 1550 (1963).

¹⁸M. Cardona, in *Solid State Physics*, edited by F. Seitz and D. Turnbull (Academic, New York, 1970), Suppl. Vol. 11.

¹⁹W. Paul, M. Demeis, and L. X. Finogold, in *Proceedings of the International Conference on Semiconductor Physics, Exeter, 1962*, (Institute of Physics and the Physical Society, London, 1963), p. 172.

²⁰J. Feinleib, W. J. Scouler, J. O. Dimmock, J. Hams, T. B. Reed, and C. R. Pidgeon, *Phys. Rev. Lett.* **22**,

1385 (1969).

²¹J. W. Allen, in *Magnetic Oxides*, edited by D. J. Craik (Wiley, New York, 1975), p. 349.

²²D. Adler and J. Feinleib, *Phys. Rev. B* 2, 3112 (1970).

²³F. Brown, C. Gahwiller, A. B. Kunz, and N. O. Lipari, *Phys. Rev. Lett.* 25, 927 (1970).

²⁴F. Brown, C. Gahwiller, and A. B. Kunz, *Solid State Commun.* 9, 487 (1971).